Simulations of Organic Aerosol Concentrations in Mexico City Using the WRF-CHEM Model during the MCMA-2006/MILAGRO Campaign

Guohui Li[(1,2)*], M. Zavala[(1)], W. Lei[(1,2)], A. P. Tsimpidi[(3,4)], V. A. Karydis[(3,4)], S. N. Pandis[(3,5)], M. R. Canagaratna[(6)], and L. T. Molina[(1,2)]

(1) Molina Center for the Energy and the Environment, La Jolla, CA, USA
(2) Massachusetts Institute of Technology, Cambridge, MA, USA
(3) Department of Chemical Engineering, University of Patras, Patras, Greece
(4) Institute of Chemical Engineering and High Temperature Chemical Processes, Foundation of Research and Technology Hellas, Patras, Greece
(5) Department of Chemical Engineering, Carnegie Mellon University, Pittsburgh, PA, USA
(6) Aerodyne Research Inc, Billerica, MA, USA

[*] Correspondence to: G. Li (lgh@mce2.org) and L.T. Molina (ltmolina@mit.edu)

Supplementary Information Section

The supplementary information (SI) provides additional description about the modeling approach used in this study. The main references include Dzepina et al. (2009), Hodzic et al. (2009, 2010), Hildebrandt et al. (2009), and Tsimpidi et al. (2010). In addition, we have also provided a table (Table SI-1) defining the terms and acronyms used for organic compounds.

Section SI-1: Gas-particle Partitioning

In the present study, the gas-particle partitioning of any SVOC is calculated based on the assumption that the bulk gas and particle phases are in equilibrium and that all condensable organics form a pseudo-ideal solution (Odum et al., 1996), which is reasonable based on the time scales of gas-particle equilibrium for submicron particles (Seinfeld and Pandis, 2006). According to Donahue et al. (2006), considering a certain mass concentration of condensed-phase organic mass, C_{OA}, a partitioning coefficient $X_{p,i}$ can be defined for condensable compound i:

$$X_{p,i} = \left(1 + \frac{C_i^*}{C_{OA}}\right)^{-1} \quad (1)$$

where C_i^* (μg m^{-3}) is the effective saturation concentration of condensable compound i. It is worthy to note that Pankow (1994) defined the absorption partitioning coefficient $K_{om,i}$ as:

$$K_{om,i} = \frac{1}{\zeta_i C_i^*} \quad (2)$$

where ζ_i is the activity coefficient of condensable species i in the absorbing organic phase. Therefore, deviation from the above gas-particle partitioning theory may occur if the organic solution is not ideal, such as near sources in urban environments with a large amount of freshly emitted particles. Given the large uncertainties in the SOA models, the non-ideal effects are not expected to dominate the prediction uncertainties (Dzepina et al., 2009).

The temperature dependence of saturation concentrations is calculated by the Clausius-Clapeyron equation:

$$C_i^* = C_{i,o}^* \frac{T_0}{T} \exp\left[\frac{\Delta H_{vap}}{R}\left(\frac{1}{T_0} - \frac{1}{T}\right)\right] \quad (3)$$

where C_i^* (μg m^{-3}) and $C_{i,o}^*$ (μg m^{-3}) are the effective saturation concentrations of condensable compound *i* at temperature *T* (K) and at reference temperature T_0 (K), respectively, ΔH_{vap} (kJ mol^{-1}) is the enthalpy of vaporization and *R* is the ideal gas constant.

Section SI-2: SOA Models

In the present study, we have used two approaches to investigate the SOA formation based on the SAPRC 99 chemical mechanism. Nine SAPRC surrogate VOCs are considered as the SOA precursors. These lumped compounds are listed in Table SI-2, together with the reactions to form the SVOCs and the rate constants. The T2-SOA model employs a traditional 2-product method to predict the SOA production from VOCs. The mass-based stoichiometric yield coefficients, the effective saturation concentrations, and molecular weight of SVOCs at 298 K are listed in Table SI-3. In the NT-SOA model, the SOA formation from the oxidation of VOCs is predicted using four SOA species whose effective saturation concentrations at 298 K are 1, 10, 100, and 1000 μg m^{-3}, respectively, instead of the traditional 2-product parameterization. In addition, the SOA yield from VOCs is NO_x-dependent. The high-NO_x and low-NO_x yields are listed in the Table SI-4. For the SOA yield branching from high-NO_x and low-NO_x conditions, we first calculate the loss rate of RO_2 radicals due to their reactions with NO and NO_3 (defined as LR_N), and the loss rate of RO_2 radicals due to self reactions and their reactions with peroxy

radicals (defined as LR_O). If the high-NO_x yield is α_{high} and the low-NO_x yield is α_{low}, the SOA yield α is calculated as:

$$\alpha = \alpha_{high} \frac{LR_N}{LR_N + LR_O} + \alpha_{low} \frac{LR_O}{LR_N + LR_O} \quad (4)$$

Figure SI-1 shows the variation of the SOA mass yield from toluene (major component of ARO1 in SAPRC 99) with the total organic aerosol concentration (C_{OA}) in the T2-SOA and NT-SOA models under high NO_x conditions. The SOA mass yield used in the NT-SOA model is higher than that in the T2-SOA model and when COA is equal to 10 μg m^{-3}, the SOA mass yield used in the NT-SOA model is about 4 times higher than that in the T2-SOA model. Detailed discussions can be found in Hildebrandt et al. (2009).

Section SI-3: POA Emissions

The MCMA 2006 official emission inventory is used in the simulations and the POA emissions are modified and distributed by volatility based on dilution experiments for the non-traditional SOA model to account for the primary organic emissions (Tsimpidi et al., 2010). The primary organic emissions must include the emitted primary organic aerosols before their dilution in the atmosphere. However, the current POA emission inventory as described above is based on ambient measurements at an urban site; according to the volatility theory, part of the emitted POA has already evaporated and is excluded from the official emission fluxes. Laboratory experiments, in which diesel exhaust and wood smoke emissions were measured at different levels of dilution, have demonstrated that the measured primary organic aerosols in ambient conditions represent 15-40% of the primary organic aerosol actually emitted, depending on the ambient organic aerosol concentration and temperature (Lipsky and Robinson, 2006). Thermal denuder measurements in Mexico City during MILAGRO (Huffman et al., 2009;

Dzepina et al., 2009) have also shown that POA in Mexico City is semivolatile. The average concentration of the organic aerosols in Mexico City was in the range of 20 μg m^{-3} during the MCMA-2003 campaign (Salcedo et al., 2006). In this range of organic aerosol ambient concentrations, the measured organic particle material is approximately one third of the total emitted organic aerosols (Fig. 1a of Robinson et al., 2007). Therefore, in order to estimate the total semivolatile organic emissions, the OA particulate inventory is multiplied by a factor of 3. Source test data for wood combustion, gasoline vehicles and diesel vehicles which used a sample train of quartz filters in combination with denuders and/or bents (Schauer et al., 1999, 2001, 2002) have shown that the mass of unmeasured IVOC vapors is between 0.25 to 2.8 times the existing primary OA emissions. In the present study, the OA emissions were distributed by volatility (Table SI-5) using the volatility distributions of Shrivastava et al. (2008). This distribution was derived by fitting gas particle partitioning data for diesel exhaust and wood smoke assuming that the mass of unmeasured IVOC emissions is equivalent to 1.5 times the primary organic aerosol emissions. The total amount of material (POA+SVOC+IVOC) introduced in the model is 7.5 times the particle-phase POA emissions in the original (not corrected for dilution effects) inventory, which is similar to the factor calculated from partitioning theory and ambient data by Dzepina et al. (2009). Several studies about OA simulations in Mexico City have been used the method to modify the POA emissions suitable for the non-traditional SOA model (Dzepina et al., 2009; Tsimpidi et al., 2010; Hodzic et al., 2010).

Supplementary Information Reference

Donahue, N. M., Robinson, A. L., Stanier, C. O., and Pandis, S. N.: Coupled partitioning, dilution, and chemical aging of semivolatile organics, Environ. Sci. Technol., 40, 2635–2643, 2006.

Dzepina, K., Volkamer, R. M., Madronich, S., Tulet, P., Ulbrich, I. M., Zhang, Q., Cappa, C. D., Ziemann, P. J., and Jimenez, J. L.: Evaluation of new secondary organic aerosol models for a case study in Mexico City, Atmos. Chem. Phys., 9, 5681–5709, 2009.

Hildebrandt, L., Donahue, N. M., and Pandis, S. N.: High formation of secondary organic aerosol from the photo-oxidation of toluene, Atmos. Chem. Phys., 9, 2973–2986, 2009.

Hodzic, A., Jimenez, J. L., Madronich, S., Aiken, A. C., Bessagnet, B., Curci, G. , Fast, J., Lamarque, J. F., Onasch, T. B., Roux, G., and Ulbrich, I. M.: Modeling organic aerosols during MILAGRO: application of the CHIMERE model and importance of biogenic secondary organic aerosols, Atmos. Chem. Phys., 9, 6949–6982, 2009.

Hodzic, A., Jimenez, J. L., Madronich, S., Canagaratna, M. R., DeCarlo, P. F., Kleinman, L., and Fast, J.: Modeling organic aerosols in a megacity: potential contribution of semi-volatile and intermediate volatility primary organic compounds to secondary organic aerosol formation, Atmos. Chem. Phys., 10, 5491–5514, 2010.

Grieshop, A. P., Logue, J. M., Donahue, N. M., and Robinson, A. L.: Laboratory investigation of photochemical oxidation of organic aerosol from wood fires 1: measurement and simulation of organic aerosol evolution, Atmos. Chem. Phys., 9, 1263–1277, 2009.

Huffman, J. A., Docherty, K. S., Mohr, C., Cubison, M. J., Ulbrich, I. M., Ziemann, P. J., Onasch, T. B., and Jimenez, J. L.: Chemically-resolved volatility measurements of organic aerosol from different sources, Environ. Sci. Technol., 43, 5351–5357, 2009.

Lipsky, E. M. and Robinson, A. L.: Effects of dilution on fine particle mass and partitioning of semivolatile organics in diesel exhaust and wood smoke, Environ. Sci. Technol., 40, 55–162, 2006.

Odum, J. R., Hoffman, T., Bowman, F., Collins, D., Flagan, R. C., and Seinfeld, J. H.: Gas/particle partitioning and secondary organic aerosol yields, Environ. Sci. Technol., 30, 2580–2585, 1996.

Pankow, J. F.: An absorption model of gas/particle partitioning involved in the formation of secondary organic aerosol, Atmos. Environ., 28, 189–193, 1994.

Robinson, A. L., Donahue, N.M., Shrivastava, M. K.,Weitkamp, E. A., Sage, A. M., Grieshop, A. P., Lane, T. E., Pandis, S. N., and Pierce, J. R.: Rethinking organic aerosols: semivolatile emissions and photochemical aging, Science, 315, 1259–1262, 2007.

Salcedo, D., Onasch, T. B., Dzepina, K., Canagaratna, M. R., Zhang, Q., Huffman, J. A., DeCarlo, P. F., Jayne, J. T., Mortimer, P., Worsnop, D. R., Kolb, C. E., Johnson, K. S., Zuberi, B., Marr, L. C., Volkamer, R., Molina, L. T., Molina, M. J., Cardenas, B., Bernab, R. M., Mrquez, C., Gaffney, J. S., Marley, N. A., Laskin, A., Shutthanandan, V., Xie, Y., Brune, W., Lesher, R., Shirley, T., and Jimenez, J. L.: Characterization of ambient aerosols in Mexico City during the MCMA-2003 campaign with Aerosol Mass Spectrometry: results

from the CENICA Supersite, Atmos. Chem. Phys., 6, 925–946, 2006, http://www.atmos-chem-phys.net/6/925/2006/.

Schauer, J. J., Kleeman, M. J., Cass, G. R., and Simoneit, B. R.T.: Measurement of emissions from air pollution sources, 2. C-1 through C-30 organic compounds from medium duty diesel trucks, Environ. Sci. Technol., 33, 1578–1587, 1999.

Schauer, J. J., Kleeman, M. J., Cass, G. R., and Simoneit, B. R. T.: Measurement of emissions from air pollution sources, 3. C-1-C-29 organic compounds from fireplace combustion of wood, Environ. Sci. Technol., 35, 1716–1728, 2001.

Schauer, J. J., Kleeman, M. J., Cass, G. R., and Simoneit, B. R. T.: Measurement of emissions from air pollution sources, 5. C-1-C-32 organic compounds from gasoline-powered motor vehicles, Environ. Sci. Technol., 36, 1169–1180, 2002.

Seinfeld, J. H. and Pandis, S. N.: Atmospheric Chemistry and Physics: From air Pollution to Climate Change, Second Edition, Wiley-Interscience, New York, 2006.

Shrivastava, M. K., Lane, T. E., Donahue, N. M., Pandis, S. N., and Robinson, A. L.: Effects of gas-particle partitioning and aging of primary emissions on urban and regional organic aerosol concentrations, J. Geophys. Res., 113, D18301, doi:10.1029/2007JD009735, 2008.

Tsimpidi, A. P., Karydis, V. A., Pandis, S. N., Zavala, M., Lei, W., and Molina, L. T.: Evaluation of the Volatility Basis-Set Approach for Modeling Primary and Secondary Organic Aerosol in the Mexico City Metropolitan Area, Atmos. Chem. Phys., 10, 525–546, 2010.

Table SI-1 The terminology used for the various fractions and sources of organic compounds.

Gas-phase organic compounds (Same as Tsimpidi et al. (2010))	
VOC	Volatile Organic Compounds: gas-phase organic species, in all cases of high volatility (e.g. toluene, isoprene, terpenes).
SVOC	Semi-Volatile Organic Compounds: species which have sufficiently low vapor pressure and are likely to dynamically partition between the gas and the aerosol phases.
POG	SVOC, emitted or formed due to evaporation of POA in the atmosphere (Robison et al., 2007)
OPOG	Oxidized POG by OH
IVOC	Intermediate Volatility Organic Compounds: organic species which have high enough vapor pressure to reside almost completely in the gas phase, but which have lower vapor pressure than the traditional VOCs (Robinson et al., 2007)
Condensed-phase organic species (Same as Hodzic et al. (2010))	
OA	Organic Aerosol: includes both primary and secondary fractions. It includes carbon mass (OC) and also the oxygen, hydrogen, and nitrogen mass which is part of OA.
TOA	Total Organic Aerosol
POA	Primary Organic Aerosol
SOA	Secondary Organic Aerosol (from all sources)
Aerosol Mass Spectrometer specific terminology (Same as Hodzic et al. (2010))	
AMS	Aerodyne Aerosol Mass Spectrometer
PMF	Positive Matrix Factorization: a mathematical factorization method applied to AMS time-dependent spectra that allows determining the contribution of different OA components to total OA mass as a function of time (Ulbrich et al., 2009, and references therein).
HOA	Hydrocarbon-like Organic Aerosols: an OA component identified with PMF which is consistent with mass spectral signatures of reduced species such as those from motor vehicle emissions. It is generally understood as a surrogate for urban combustion-related POA (Aiken et al., 2009a, and references therein).
OOA	Oxygenated Organic Aerosols: an OA component identified with PMF which is characterized by its high oxygencontent. It is generally understood as a surrogate for SOA from all sources.
BBOA	Biomass Burning Organic Aerosols: an OA component identified with PMF which is characterized by spectral features typical of biomass smoke. It is thought to be dominated by biomass burning POA, while biomass burning SOA is mostly apportioned into the OOA component.

Table SI-2 Lumped compounds considered as SOA precursors, the reactions to form SVOCs and the rate constants.

Species	Major Components	Reactions	Rate Constant (298 K) (cm^3 $molec^{-1}$ s^{-1})
ALK4	C_5-C_6 Alkanes, Cyclopetane, Trimethyl Butane, Trimethyl Pentane, Isopropyl Alcohol, n-Propyl Alcohol	ALK4 + OH	4.39×10^{-12}
ALK5	C_7-C_{22} n-Alkanes, C_6-C_{16} Cycloalkanes, Branched/Unspeciated C8-C18 Alkanes	ALK5 + OH	9.34×10^{-12}
OLE1	Propene, C_4-C_{15} Terminal Alkenes	OLE1 + OH OLE1 + O_3 OLE1 + NO_3	3.23×10^{-11} 1.06×10^{-17} 1.26×10^{-14}
OLE2	Isobutene, C_4-C_{15} Internal Alkenes, C_6-C_{15} Cyclic or di-olefins, Styrenes	OLE2 + OH OLE2 + O_3 OLE2 + NO_3	6.33×10^{-11} 1.07×10^{-16} 7.27×10^{-13}
ARO1	Toluene, Benzene, Ethyl Benzene, C_9-C_{13} Monosubstituted Benzenes	ARO1 + OH	5.95×10^{-12}
ARO2	Xylenes, Ethyl Toluenes, Dimethyl and Trimethyl Benzenes, Ethylbenzenes, Naphthalene, C_8-C_{13} Di-, Tri-, Tetra-, Penta-, Hexa-substituted Benzenes, Unspeciated C_{10}-C_{12} Aromatics	ARO2 + OH	2.64×10^{-11}
CRES	Cresols	CRES + OH CRES + NO_3	4.20×10^{-11} 1.37×10^{-11}
ISOP	Isoprene	ISOP + OH ISOP + O_3	9.82×10^{-11} 1.28×10^{-17}
TERP	α-pinene, β -pinene, Limonenene, Carene, Sabinene, other monoterpenes	TERP + OH TERP + NO_3 TERP + O_3 TERP + $O(^3P)$	8.27×10^{-11} 6.57×10^{-12} 6.88×10^{-17} 3.27×10^{-11}

Table SI-3 Parameters used in the T2-SOA model.

SOA Precursors	**$SVOC_1$**		**$SVOC_2$**		**Molecular Weight** ($g\ mol^{-1}$)
	α ($\mu g\ m^{-3}/\mu g\ m^{-3}$)	C^* ($\mu g\ m^{-3}$)	α ($\mu g\ m^{-3}/\mu g\ m^{-3}$)	C^* ($\mu g\ m^{-3}$)	
ALK4	-	-	-	-	-
ALK5	0.0718	0.3103	-	-	150
OLE1	-	-	-	-	-
OLE2	0.36	111.11	0.32	1000.0	150
ARO1	0.071	1.716	0.138	47.855	150
ARO2	0.038	2.165	0.167	64.946	150
CRES	0.05	0.2611	-	-	150
ISOP	-	-	-	-	-
TERP	0.0864	0.865	0.3857	11.804	177

Table SI-4 SOA yield scenarios using a four-product basis set with saturation concentrations of 1, 10, 100, and 1000 μg m^{-3} at 298 K.

SOA Precursors	Aerosol Yield* High-NOx Parameterization				Aerosol Yield High-NOx Parameterization				Molecular Weight
	1	10	100	1000	1	10	100	1000	(g mol^{-1})
ALK4	0.000	0.038	0.000	0.000	0.000	0.075	0.000	0.000	120
ALK5	0.000	0.150	0.000	0.000	0.000	0.300	0.000	0.000	150
OLE1	0.001	0.005	0.038	0.150	0.005	0.009	0.060	0.225	120
OLE2	0.003	0.026	0.083	0.270	0.023	0.044	0.129	0.375	120
ARO1	0.003	0.165	0.300	0.435	0.075	0.225	0.375	0.525	150
ARO2	0.002	0.195	0.300	0.435	0.075	0.300	0.375	0.525	150
CRES	-	-	-	-	-	-	-	-	-
ISOP	0.001	0.023	0.015	0.000	0.009	0.030	0.015	0.000	136
TERP	0.012	0.122	0.201	0.500	0.107	0.092	0.359	0.600	180

* The SOA yields are based on an assumed density of 1.5 g cm^{-3}.

Table SI-5 Parameters used to treat partitioning of POA emissions.

C^* at 298K ($\mu g\ m^{-3}$)	0.01	0.1	1	10	10^2	10^3	10^4	10^5	10^6
Fraction of emissions	0.03	0.06	0.09	0.14	0.18	0.30	0.40	0.50	0.80
Emission Phase (Particle: P; Gas: G)	P	P	P	P	P	P	G	G	G
Molecular Weight ($g\ mol^{-1}$)	250	250	250	250	250	250	250	250	250
$\triangle H$ ($kJ\ mol^{-1}$) (Robinson et al., 2007)	112	106	100	94	88	82	76	70	64
$\triangle H$ ($kJ\ mol^{-1}$) (Grieshop et al., 2009)	77	73	69	65	61	57	54	50	46

Supplementary Information Figure Captions

Figure SI-1: The SOA mass yield from toluene (y-axis) with the total organic aerosol concentration (x-axis) under high NO_x conditions. Blue line: used in the T2-SOA model; Red line: used in the NT-SOA model.

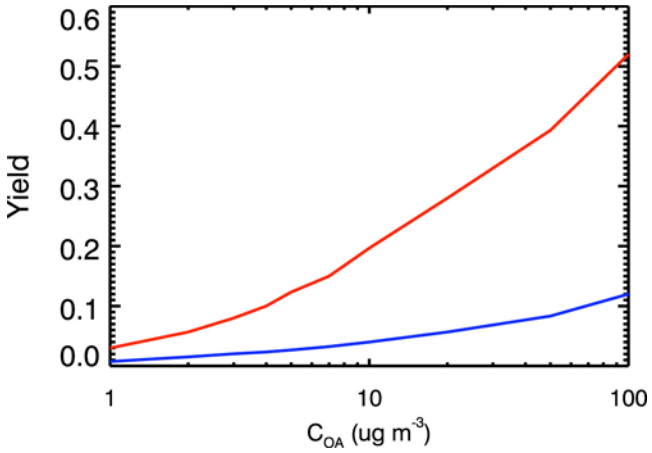

Figure SI-1